

# Bonded Ceramic-Metal Layers for Fabrication of Thermal Conduction Plates

Madhav Datta

**Abstract**—The work described in this article is part of an effort to build reliable and efficient liquid cooling modules for high-power laser diodes. The cooling system is designed to mount at least 12 laser diodes to a common microheat exchanger, thus requiring a large-size thermal conduction plate. Fabrication of the thermal conduction plate involved void-free bonding of copper layers on both sides of an aluminum nitride (AlN) plate. In the current study, ceramic-metal bonding methods using moly-manganese metallization and active metal brazing were investigated. Bonded AlN/copper plates were characterized and evaluated by optical microscopy, scanning electron microscopy, and energy dispersive spectrometry. For detecting voids, cracks, and delamination, some of the plates were analyzed by scanning acoustic microscopy (C-SAM). Results indicated that >99% void-free bonded AlN/Cu plates can be fabricated by using properly selected metallization conditions and brazing temperature profiles. The active metal brazing approach was found to be a cost-effective method of fabricating reliable, void-free thermal conduction plates.

**Keywords**—Thermal conduction plate, liquid cooling module, aluminum nitride, metal-ceramic bonding, laser diode cooling, void-free bonding, active metal brazing, MoMn metallization

## INTRODUCTION

Miniaturization of performance-driven high-power electronic devices and packages is leading to large heat fluxes at the chip. Cooling such high-power devices is beyond the capability of conventional cooling solutions. To remove heat generated in power semiconductor modules, a liquid-cooled cold plate offers a solution that reduces the barrier to heat flow while maintaining mechanical integrity of the package [1]. Liquid cooling is becoming increasingly important for effective cooling of high-power laser diodes and power conversion devices such as isolated gate bipolar transistors.

A typical laser diode liquid-cooling assembly is shown in Fig. 1 [2]. The cooling assembly consists of two key components: (1) a thermal conduction plate with at least 12 conducting pads to which the laser diodes are mounted and (2) a microheat exchanger containing high surface-to-volume ratio microstructure (HSVRM) [1]. The thermal conduction plate is joined to the microheat exchanger. The heat generated in

the laser bar conduction plate is extracted by flowing a cooling liquid through the microheat exchanger.

## THERMAL CONDUCTION PLATE

Thermal conduction plate is one of the key components of the liquid cooling assembly described previously [3]. The process of making a thermal conduction plate involves bonding a ceramic plate with copper layers on both sides. The next step is the photopatterning of copper layers to form electrically isolated copper pads on which the laser diodes are joined. This photopatterning includes selective removal of copper and the joining material through patterned photoresist and can be accomplished by wet etching and/or physical methods. The final step is laser machining to provide drilled alignment holes and final shaping of the plate.

The ceramic substrate of the conduction plate must possess high thermal conductivity and high electrical resistivity. Since multiple (12) devices are mounted on the thermal conduction plate, large ceramic substrates of the order of 160 mm × 50 mm × 0.6 mm are used. The thermal conduction plate must be mechanically robust, and it should exhibit minimum warpage. All of these requirements pose challenges in fabricating the conduction plate. In an effort to build reliable liquid cooling modules for high-power laser diodes, different methods of bonding Cu/ceramic/Cu layers were investigated in this study.

### A. Choice of Ceramic Substrate

Packaging materials for high-power density devices must offer effective thermal management as well as excellent mechanical stability. Ceramic materials are best suited for such applications, and the choice of the right ceramic material often involves determining the best trade-off between price and performance. Among many ceramic materials that are commercially available today, alumina (Al<sub>2</sub>O<sub>3</sub>), aluminum nitride (AlN), and beryllium oxide (BeO) are the more favored substrates used in manufacturing power devices. Table I compares the room-temperature physical properties of ceramic materials applicable in power devices [4, 5]. Al<sub>2</sub>O<sub>3</sub> has been widely used as a substrate material in hybrid microcircuits for many decades due to its low cost. However, the low thermal conductivity of Al<sub>2</sub>O<sub>3</sub> at about 30 W/mK makes it less suitable for high-power applications. AlN and BeO materials, each offer a set of benefits and shortcomings for high-power packaging applications. The thermal conductivity of AlN is ~185 W/mK

The manuscript was received on March 25, 2015; revision received on May 29, 2015; accepted on May 29, 2015

Department of Chemical Engineering and Materials Science, and Amrita Center for Industrial Research and Innovations, Amrita University, Coimbatore, Tamil Nadu 64112, India  
email: madhavdatta@cb.amrita.edu

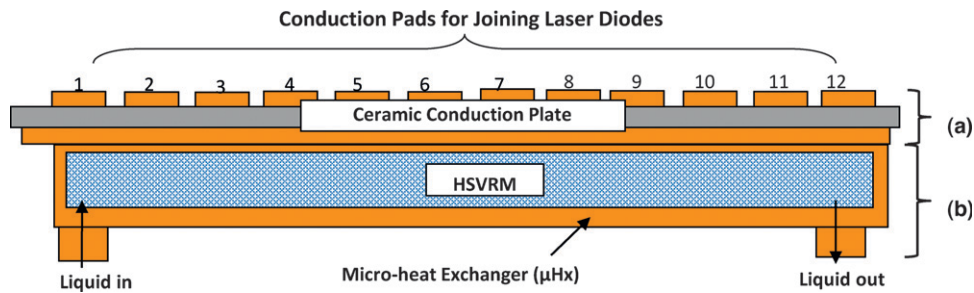


Fig. 1. Liquid-cooling module for cooling laser diodes. The cooling module is designed to mount 12 laser diodes on the same microheat exchanger. Laser diodes are mounted on patterned copper pads of a thermal conduction ceramic plate (a) which is joined to a microheat exchanger (b) with active high surface to volume ratio material, HSVRM.

Table I  
Thermoelectrical Properties of Different Materials at Room Temperature [4,5]

Material	Thermal conductivity (W/mK)	Electrical resistivity ( $\Omega\cdot\text{m}$ )	CTE (ppm/ $^{\circ}\text{C}$ )
$\text{Al}_2\text{O}_3$	30	$>10^{11}$	7.3
AlN	185	$>10^{11}$	4.5
BeO	285	$>10^{11}$	8.0
SiC diamond	550–650	$>10^{11}$	2.0
Si	149	$2.3 \times 10^{-3}$	3.3
Cu	390	$1.7 \times 10^{-8}$	16.6

while that for BeO is  $\sim 285$  W/mK. However, BeO is also the most expensive of the three materials. Furthermore, BeO may pose a health risk if recommended safe handling practices are not followed; the inhalation of airborne BeO containing particles may cause a serious lung disorder in susceptible individuals. Due to these reasons, packages containing BeO substrates pose shipping and disposal restrictions, particularly in Japan and European countries. SiC diamond, although having the highest thermal conductivity among the materials shown in Table I, has not been considered because it is prohibitively expensive for the present application.

Another parameter to consider is the coefficient of thermal expansion (CTE), which indicates how the size of a material changes with temperature, in parts per million (ppm) per change in temperature in degree centigrade ( $^{\circ}\text{C}$ ). Most materials will expand with increasing temperature, so the change is unavoidable. Because semiconductor devices are joined to a package substrate by soldering or by epoxy, ideally the CTE of the package material should be matched to that of the semiconductor chip so that both materials can expand and contract equally during thermal excursions. Among the ceramic materials considered in Table I, the CTE of AlN at about 4.5 ppm/ $^{\circ}\text{C}$  is well matched for Si at 3.3 ppm/ $^{\circ}\text{C}$ . Considering cost, thermal conductivity, toxicity, and CTE parameters, AlN substrates are considered to be the ceramic material of choice for fabrication of thermal conduction plates.

AlN hydrolyzes in a water-containing environment [6], which results in the reduction of its thermal conductivity by oxygen contamination in AlN grains [7, 8]. Oxygen contamination arises not only from the powder manufacturing process, but also from contact with water molecules in powder processing after manufacturing. From the point of view of this

study, the exposure of AlN substrates to the atmospheric humidity and its reactivity during brazing operation is of interest. According to Abid et al. [9], AlN does not readily react with atmospheric moisture at room temperature. Also, different studies have confirmed that the formation of a protective oxide layer on the surface of AlN powder at elevated temperatures can hinder the hydrolysis process [10, 11]. Due to these reasons, the possibility of AlN hydrolysis during brazing operation at high temperatures and its possible influence on the bonding process was considered to be minimal to nonexistent in this study.

### B. Ceramic/Metal Bonding

A ceramic thermal conduction plate must have a highly conductive metal layer in order to be used in the assembly of power devices. Normally, copper with a thickness ranging up to millimeters is chosen for this layer. The copper layer must be adherent to the ceramic substrate, and the entire ensemble should possess the high thermal conductivity necessary for dissipation of heat in electronic power modules. Due to the inherent property of the nonwetting characteristics of ceramic materials, bonding metal to ceramic and fabricating patternable, high-yielding, void-free bonded ceramic-copper plates are challenging tasks. Several methods employed for bonding metal to ceramic substrates include the use of direct bonding, moly-manganese metallization, and active brazing materials.

Direct-bonded copper (DBC) is a high-temperature oxidation process to bond a sheet of copper to one or both sides of a ceramic plate. The assembled ceramic plate and copper sheet(s) are heated in the temperature range of 1,065 $^{\circ}\text{C}$  to 1,080 $^{\circ}\text{C}$  in an atmosphere of nitrogen containing about 30 ppm of oxygen [12]. Under these conditions, a copper-oxygen eutectic forms, which bonds both to copper and the substrate. The composition of the bonding atmosphere is very important since the initially formed  $\text{Cu}_2\text{O}$  must be maintained. If the oxygen partial pressure is too high, all copper is converted to eutectic melt; conversely, if the partial pressure is less than the equilibrium partial pressure, the oxide is reduced and the eutectic phase will not form [13]. Other approaches include implantation of ions such as oxygen, titanium, and iron ions into AlN substrates and preoxidation of copper [14, 15]. The DBC is characterized by the absence of an intermediate layer at the metal-ceramic interface, which provides good thermal conductivity at the metal-ceramic junction. Direct bonding methods permit bonding of substantially thick metal layers.

A serious drawback associated with DBC is that large area metal-ceramic bonds cannot be reproducibly formed without the occurrence of blisters in the metal-ceramic interface. Blisters are believed to be due to the entrapment of gases or the evolution of gases from contaminants during the direct-bonding operation. Blistering lowers thermal dissipation and reliability of electrical contacts through the assembly due to discontinuity at the metal-ceramic interface. For DBC on BeO, the substrate area to which metal can be reproducibly direct-bonded without blistering is limited to less than 1 in<sup>2</sup>. For AlN, however, the DBC process yields very poor peel strength [16].

The Moly-manganese metallization process is another commonly employed method for bonding metal to ceramic substrates. This method typically requires the formation of an intermediate bonding layer consisting of a slurry of powdered Mo and Mn mixed with glass additives (such as Fe, Si, TiO<sub>2</sub>, Al<sub>2</sub>O<sub>3</sub>, and CaO) and volatile carriers deposited on the ceramic plate [17-19]. The deposited layer is bonded to the ceramic plate by heating in a wet hydrogen furnace. The fired coating is subsequently coated with a layer of electroless nickel. The moly-manganese metallized ceramic plate thus formed can then be given a bonded conductive copper layer either by electroplating or by brazing a copper sheet.

Active metal brazing (AMB) permits metals to be joined to ceramics without the need for metallization of the ceramic surface [20-22]. AMB requires an active element that will react with the ceramic, forming a reaction layer between the ceramic and the molten brazing material that will reduce the interfacial energy to such a level that wetting of the ceramic occurs. The active elements used for this process include Ti, Zr, Hf, V, and Al. The best known of these active elements is Ti, which is used in many commercially available braze alloys. AMB alloys are mainly based on Ag, In, Cu, or Ag-Cu eutectic systems with added Ti. The brazing operation is usually performed in an inert or ultrahigh vacuum environment. High-vacuum or inert atmospheres are required because excessive oxygen in the atmosphere can react with the active element in the active braze filler metal and compromise joint strength and integrity [22]. The cost of AMB materials varies significantly depending on the presence or absence of silver and indium in the alloys. Cu-ABA is the most cost-effective of all the commercially available active brazing materials.

## MATERIALS AND TECHNIQUES

AlN ceramic material used in this study contained 4% Y<sub>2</sub>O<sub>3</sub> as a sintering aid. Lapped and cleaned AlN plates, 165 mm × 51 mm × 0.6 mm in size, were supplied by P/M Industries (Portland, OR); as-received plates were used without any surface treatment. Electronic grade, oxygen-free high conductivity copper 101 sheets, 165 mm × 51 mm in size, were cut from a stock of 0.3-mm-thick roll. CuSil shims, 0.25 mm thick, were obtained from Prince Iznat Co. (Cleveland, OH); and 0.05-mm-thick shims of active brazing material, Cu-ABA was supplied by Morgan Advanced Ceramics (Hayward, CA). Copper, CuSil, and Copper ABA parts were cleaned with alcohol and dried before use. Composition and melting temperatures of these materials are given in Table II.

Table II  
Composition and Melting Temperatures of Copper and Brazing Alloys

Material	Composition	Temperature (°C)
Copper	OFHC Cu 101	Melting point: 1,085
CuSil	28% Cu, 72% Ag	Eutectic temperature: 780
CuABA	92.75%Cu, 3% Si, 2 % Al, 2.25% Ti	Solidus: 958, liquidus: 1,024

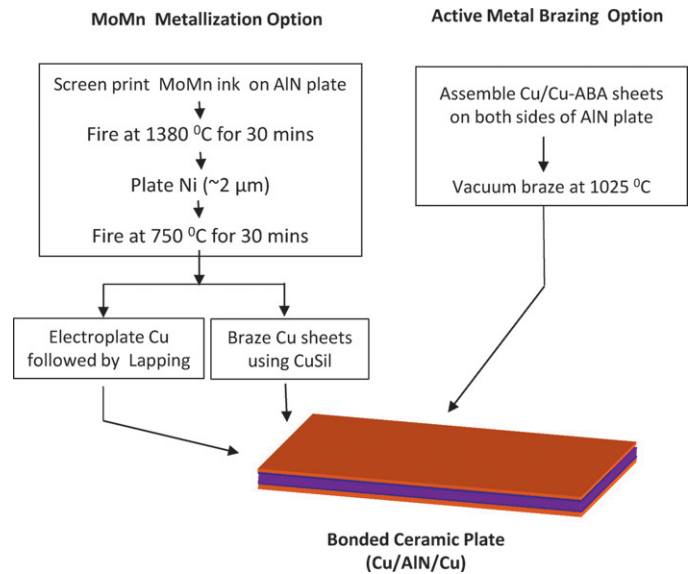


Fig. 2. Different methods and their process steps used for fabrication of bonded AlN/Cu plates.

Both moly-manganese metallization and AMB methods of fabricating conduction plates were evaluated in this study. The different approaches and their assemblies are depicted schematically in Fig. 2. Bonded ceramic/copper plates were characterized and evaluated by optical microscopy, scanning electron microscopy, and energy dispersive x-ray spectrometry. Some of the plates were analyzed by scanning acoustic microscopy (C-SAM) to detect voids, cracks, and delamination.

## EXPERIMENTAL DETAILS

For the metallization approach to fabricating the conduction plate, 10-20- $\mu$ m-thick moly-manganese ink was screen printed on the ceramic plate, and the plate was air dried. The coating was then fired at different temperatures between 1,300°C and 1,600°C in a wet hydrogen (15-30°C dew point) environment for 30 min. The fired coating was subsequently plated with a 3-5- $\mu$ m-thick electroless nickel layer. The nickel layer was sinter-fired at 750°C in a dry hydrogen (99.9%) atmosphere, leaving a finished metallic surface that could be either electroplated with a copper layer or brazed with a copper sheet using standard braze filler materials such as CuSil. For electroplating, the metallized ceramic plates were mounted on a specially designed fixture with dummy auxiliary electrodes around the plates. These dummy electrodes helped in minimizing the higher deposition rate at the edges of the plate.

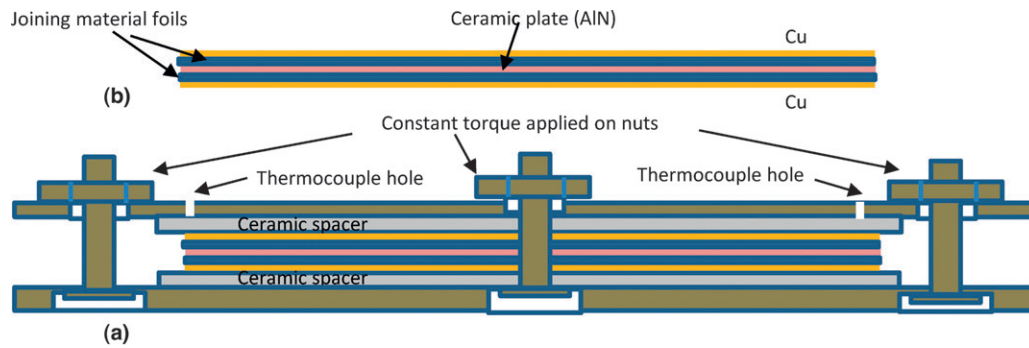


Fig. 3. Stainless steel fixture (a) used for brazing metal-ceramic sandwich (b). The sandwich was placed in between two ceramic spacers in the fixture. A constant torque was applied on six nuts that provided constant pressure on the plates during brazing. Several holes in the upper stainless plate of the fixture allowed placement of thermocouples.

The fixture was made of a cathode in an electrolytic cell containing a high-speed pyrophosphate copper plating bath. The anode material consisted of OFHC Cu101 rods contained in a titanium basket. The electrolyte was vigorously agitated with air and continuously filtered with a carbon pack. The electroplated ceramic plates required a post-lapping process to achieve a uniform desired thickness of copper over the ceramic plate.

For the brazing approach, a CuSil shim was used between the metallized ceramic plate and copper sheet. The complete assembly and the fixture used for brazing are shown in Fig. 3. The fixture consisted of two stainless steel plates with six stainless steel bolts inserted through holes in the plates. The assembled sandwich (Cu/CuSil/metallized AlN/CuSil/Cu) was placed between two boron nitride-coated thick  $\text{Al}_2\text{O}_3$  spacers. The assembled sample was pressurized by applying a constant torque of 102 Nm (75 ft-lb) to tighten the nuts in the fixture. Brazing was conducted in a forming (95%  $\text{N}_2$ /5%  $\text{H}_2$ ) gas furnace at a peak temperature of 820°C corresponding to a temperature well above the eutectic temperature of CuSil at 780°C.

For the AMB approach, a sandwich of Cu/copper ABA/AlN/copper ABA/Cu was assembled and placed in the fixture. Brazing was conducted in a vacuum furnace at a constant vacuum of  $10^{-5}$  Torr, and temperature was monitored at three different locations on the sample using thermocouples. Brazing operations were conducted at different temperatures between 975°C and 1,050°C. In order to achieve a uniform brazing temperature over the sample, a two-step temperature profile comprising two soak times was used. First, the temperature was ramped at a heating rate of 8°C/min up to an equalizing temperature (ET) approximately 40°C below the

desired brazing temperature. A 10-min soaking time was set at ET that allowed all of the thermocouple temperatures to equalize. Next, the temperature was again ramped at a heating rate of 5°C/min up to the set peak temperature (PT). At this point, a 30-min soak time allowed the peak temperature to stabilize and the brazing process to complete. A typical temperature profile for a peak brazing temperature of 1,020°C is shown in Table III. After completion of the brazing operation, the sample was vacuum cooled to 90°C before removing it from the furnace.

## RESULTS AND DISCUSSION

### A. MoMn Metallization

The MoMn metallization approach of bonding ceramic to metal is mainly used for bonding  $\text{Al}_2\text{O}_3$  substrates and is restricted to small sizes generally on the order of 25 mm × 25 mm. In this study, the use of large-sized AlN substrates posed challenges due to void formation and delamination at the ceramic/MoMn interface as determined by C-SAM analysis. In a first set of experiments, the MoMn metallization formed by firing at 1,300°C exhibited the presence of large voids that were evenly distributed over the ceramic plate with a void fraction >70%. To determine the influence of firing temperature on adhesion of the MoMn layer to AlN, further experiments were conducted at different firing temperatures between 1,300°C and 1,600°C at increments of 50°C. Increasing the firing temperature indeed led to minimized void size and void fraction. At a firing temperature >1,500°C, the AlN/MoMn interface was >96% void-free. The AlN plates with void-free MoMn metallized layers were plated with 3-5 μm electroless nickel followed by sintering at 750°C in a dry hydrogen (99.9%) atmosphere.

Electroplating 250-300-μm-thick copper on metallized AlN plates required >12 h. While the use of dummy auxiliary electrodes around the plate helped minimize excessive deposition at the edges of AlN plates, the uniformity of copper deposition across the plate was unacceptable; a post-lapping operation was required to obtain copper thickness within ±3 μm. Due to these reasons electroplating copper was considered an expensive approach of fabricating thermal conduction plates.

An alternative method of bonding copper to metallized AlN plate is brazing copper sheet by using CuSil shims as

Table III  
Temperature Profile Used for Vacuum Brazing of AlN/Cu Plates Using AMB Cu-ABA Alloy

Parameter	Equalizing temperature	Peak temperature
Temperature (°C)	980	1020
Heating rate (°C/min)	8	5
Soak time (min)	10	30
Quench method	Vacuum cooled to 90°C	
Vacuum	$10^{-5}$ Torr	

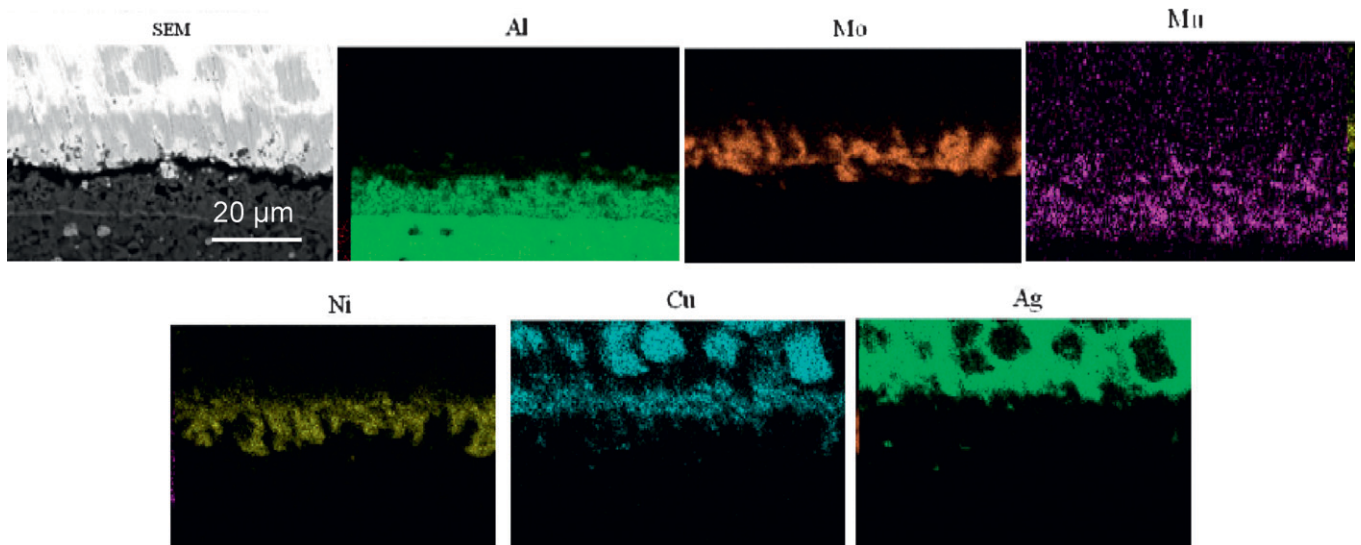


Fig. 4. Energy dispersive x-ray mapping of different elements present at the joint of a brazed MoMn metallized AlN/Cu plate using CuSil as the filler material. Mn diffuses into AlN, there is overlapping of Mo-Ni, Ni-Cu, and Cu-Ag signals indicating good bonding of AlN/Cu layers.

the filler material, as described previously in the “Experimental Details” section. A constant torque used on the nuts in the fixture exerted uniform pressure on the assembled layers during brazing, which helped to minimize voids. Fig. 4 shows energy dispersive x-ray mapping of elements at the different interfaces (AlN/MoMn/Ni/CuSil/Cu) of the brazed AlN/Cu plate. The energy dispersive x-ray data indicate that Mn in the MoMn metallized layer diffuses into the AlN surface. Also overlapping of Mo/Ni, Ni/Cu, and Cu/Ag signals are indicative of mixing of these layers, thereby leading to good ceramic-metal bonding.

### B. Active Metal Brazing

Cu-ABA was chosen from among several commercially available active brazing materials such as Cu-ABA, CuSil-ABA, and InCuSil-ABA because it is a comparatively less expensive material. Cu-ABA has a relatively high liquidus temperature of 1,024°C (Table II), and the Cu-ABA brazing process was very sensitive to the temperature profile used. Therefore, maintaining temperature uniformity across the sample was very critical. This was accomplished by using three thermocouples placed on the sample fixture in combination with a carefully designed heating temperature profile as described previously. Brazing operations were conducted at different peak temperatures between 975°C and 1,050°C. The brazed plates obtained at different peak temperatures were analyzed by C-SAM. Typical C-SAM images of the AlN/Cu interface of two plates brazed at two different brazing temperatures, 1,005°C and 1,020°C, respectively, are shown in Fig. 5. In C-SAM analysis, the images are created based on how the ultrasound transmits through the entire sample thickness. Since air space defects such as voids, delamination, cracks, and porosity cannot transmit the ultrasound waves, the loss of the transmitted signal corresponds to the presence of these types of defects. In Fig. 5 this is shown in terms of brightness versus darkness. The obtained interface data were quantified by a digital image analyzer attached to the C-SAM

equipment. The ceramic plate brazed at 1,005°C exhibited voids of different sizes over the sample with the void fraction being 61.39%, indicating poor bonding of Cu with the AlN substrate. On the other hand, the surface of the plate brazed at 1,020°C was almost void free with the void fraction being 0.69%, indicating an excellent bonding of Cu to AlN. At temperatures above 1,030°C, above the liquidus temperature of Cu-ABA, the joining material converted to a liquid form that, in some cases, oozed out of the ceramic-metal sandwich, flowing into the ceramic spacers and the fixture and leading to undesirable bonding with these materials. These results indicated that a narrow brazing temperature window exists for bonding Cu to AlN using Cu-ABA. Brazing operations conducted at just below the liquidus temperature of Cu-ABA, ~1,020°C, yielded excellent bonding with >99% void-free ceramic plates.

AlN-Cu plates brazed at 1,020°C were further analyzed by energy dispersive x-ray mapping to determine the presence of key elements and their interaction at the metal-ceramic joint. The results are shown in Fig. 6. The data presented in Fig. 6 show that the nitrogen signal extends up to titanium layer. Titanium in Cu-ABA reacts with nitrogen in AlN, thereby forming an intermetallic interfacial reaction product that wets the ceramic surface. The wetted AlN surface can then easily form a joint with the brazing alloy. Fig. 6 also shows that active brazing material Cu-ABA and Cu mix well, providing an excellent joint. These data in combination with the aforementioned C-SAM data indicate that robust, void-free AlN/Cu bonding can be obtained by AMB using Cu-ABA.

### SUMMARY AND FINAL REMARKS

The current study was aimed at developing methods to fabricate thermal conduction plates for liquid cooling modules. The thermal conduction plate required void-free bonding of copper layers on both sides of a large AlN ceramic plate. Three different ceramic-metal bonding methods involving

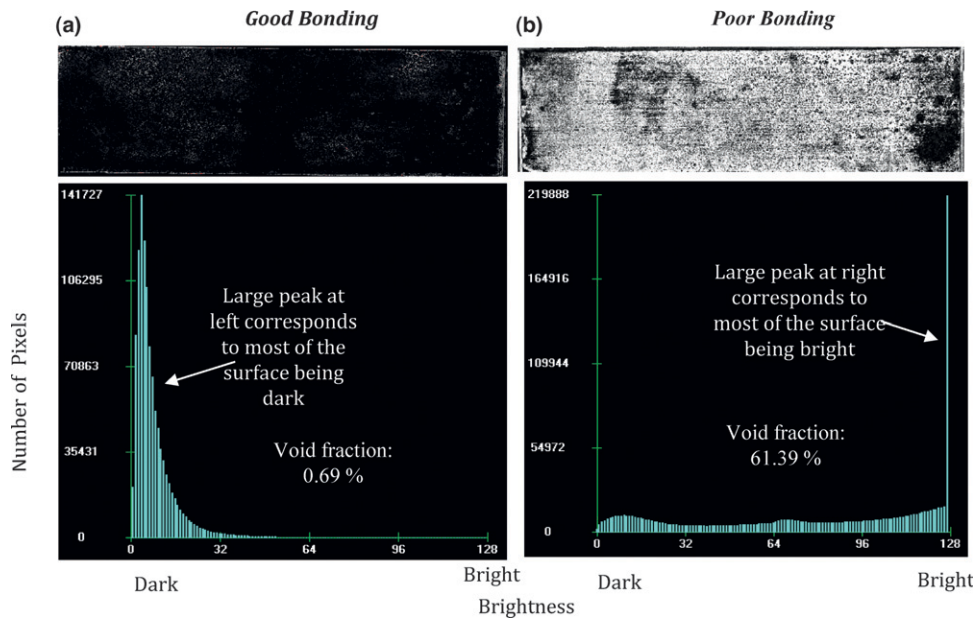


Fig. 5. C-SAM characterization of AlN/Cu plate brazed with Cu-ABA at two different temperatures. Brazing at 1,020°C provided >99% void-free bonding (a), while brazing at 1,005°C yielded poorly bonded plate with void fraction >60% (b).

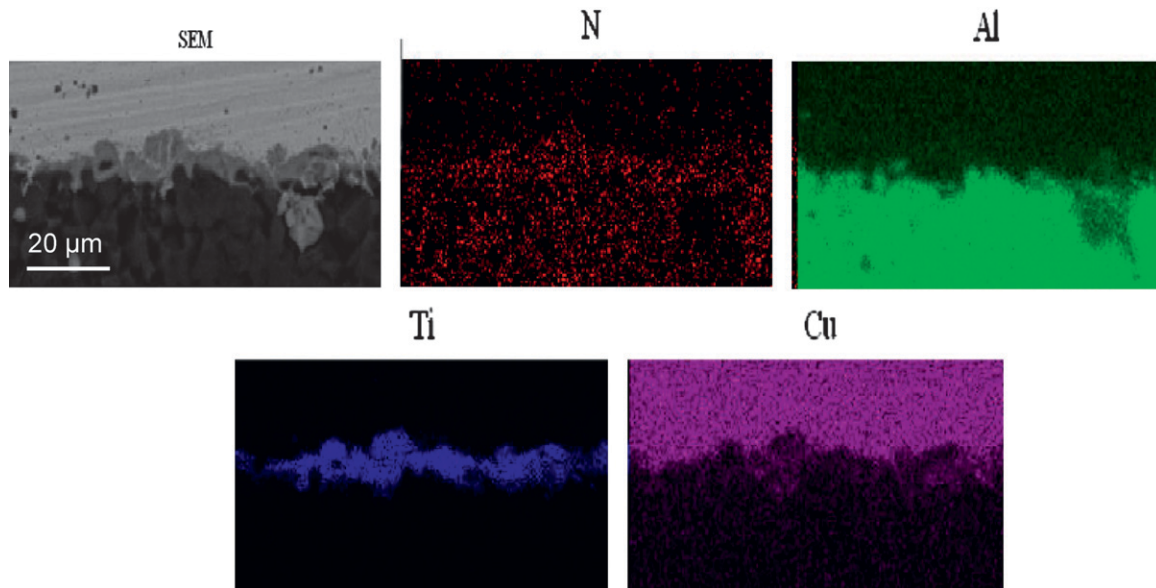


Fig. 6. Energy dispersive x-ray mapping of different elements present at the joint of brazed AlN/Cu plate using Cu-ABA brazing alloy. Nitrogen signal extends up to Ti layer indicating reaction of Cu-ABA with AlN to provide chemical bonding of Cu to AlN plate.

Table IV  
Comparison of Different Ceramic–Metal Bonding Methods Used in the Current Study

Items	MoMn metallization		
	Electroplated Cu	CuSiI brazed Cu	AMB with Cu-ABA
Process steps	Multiple	Multiple	Single
Limitations	Too many interfaces and Cu thickness variations	Too many interfaces	Narrow brazing temperature window
Concerns	Possible yield/reliability issue due to interfacial delamination and voids	Possible yield/reliability issue due to interfacial delamination and voids	Melted joining material flowing into spacers and fixture
Cost	Most expensive	Expensive	Least expensive

moly-manganese metallization and AMB were investigated. Results indicated that with careful consideration of processing parameters, each of these methods could provide void-free (void fraction <1%) bonding of large sized Cu/AlN/Cu plates. To ascertain the applicability of these methods to the large-scale fabrication of thermal conduction plates, the advantages and disadvantages of each method are compared in Table IV. The MoMn metallization process involves multiple process steps, which makes it an expensive approach. Furthermore, this approach leads to too many interfaces that are vulnerable to possible interfacial delamination and void formation, leading to possible reliability and yield issues. These factors are particularly crucial for bonding of large parts as employed in this study. For electroplated copper, the additional cost is due to the high cost of plating and lapping. AMB using Cu-ABA is the least expensive of the three methods used in this study. However, the brazing temperature window is rather narrow for this approach. With precise control of the optimum brazing temperature, AMB using Cu-ABA provides a reliable method for fabricating robust thermal conduction plates.

#### ACKNOWLEDGMENTS

The work presented in this paper was conducted at Cooligy Precision Cooling, Emerson Network Power (ENP), 800 Maude Avenue, Mountain View, CA 94034. The author thanks the ENP management for approval and permission to publish this work.

#### REFERENCES

- [1] M. Datta, E. Lin, H. Choi, M. McMaster, R. Brewer, D. Werner, J. Hom, G. Upadhyay, S. Gopalakrishnan, and F. Rebarber, "Liquid cooling system for advanced microelectronics," *ECS Transactions*, Vol. 6, No. 8, pp. 13-31, 2007.
- [2] M. Datta, B. Leong, and M. McMaster, "Microheat exchanger for laser diode cooling," US Patent No. 8254422, August 28, 2012.
- [3] M. Datta and M. McMaster, "Bonded metal and ceramic plates for thermal management of optical and electronic devices," US Patent No. 8299604, October 30, 2012.
- [4] S.L. Shinde and J. Goela, eds., *High Thermal Conductivity Materials*, Springer, New York, NY, 2006.
- [5] M. Keltner, B. Biebersmith, N. Roland, and B.K. Sharma, "Aluminum nitride vs. beryllium oxide for high power resistor products," *Microwave Journal*, 2001.
- [6] P. Bowen, J.G. Highfield, A. Mocellin, and T.A. Ring, "Degradation of aluminum powder in an aqueous environment," *Journal of the American Ceramic Society*, Vol. 73, pp. 724-728, 1990.
- [7] K. Watari, M. Kawamoto, and K. Ishizaki, "Sintering chemical reactions to increase thermal conductivity of aluminium nitride," *Journal of Materials Science*, Vol. 26, pp. 4727-4732, 1991.
- [8] K. Watari, K. Ishizaki, and T. Fujikawa, "Thermal conduction mechanism of aluminium nitride ceramics," *Journal of Materials Science*, Vol. 27, pp. 2627-2630, 1992.
- [9] A. Abid, R. Bensalem, and B.J. Sealy, "The thermal stability of aluminum nitride," *Journal of Materials Science*, Vol. 21, pp. 1301-1304, 1986.
- [10] L.M. Svedberg, K.C. Arndt, and M.J. Cima, "Corrosion of aluminum nitride (AlN) in aqueous cleaning solutions," *Journal of the American Ceramic Society*, Vol. 83, pp. 41-46, 2000.
- [11] Y. Li, T. Qiu, and J. Xu, "Effect of thermal oxidation treatment in air on the hydrolysis of AlN powder," *Materials Research Bulletin*, Vol. 32, pp. 1173-1179, 1997.
- [12] E. Entezarian and R.A. Drew, "Direct bonding of copper to aluminum nitride," *Materials Science and Engineering A*, Vol. 212, pp. 206-212, 1996.
- [13] D. Tréheux, P. Lourdin, V. Guipont, and D. Juvé, "Mechanical behavior of metal-ceramic bonds," *Journal de Physique III France*, Vol. 4, No. 10, pp. 1883-1898, 1994.
- [14] J.W. Lee, I. Radu, and M. Alexe, "Oxidation behavior of AlN substrate at low temperature," *Journal of Materials Science Materials in Electronics*, Vol. 13, No. 3, pp. 131-137, 2002.
- [15] M.G. Nicholas, ed., *Joining of Ceramics*, Chapman and Hall, London, UK, 1990.
- [16] N. Iwase, K. Anzai, K. Shinozaki, O. Hirao, T. Thanh, and Y. Siguru, "Thick film and direct bond Forming technologies for aluminum nitride substrate," *IEEE Transactions on Components, Hybrids and Manufacturing Technology*, Vol. 8 No. 2, pp. 253-258, 1985.
- [17] *Brazing Handbook*, 5th ed., pp. 462-464, 579-580, American Welding Society, Miami, FL, 2007.
- [18] G. Humpston, and D. M. Jacobson, *Principles of Soldering and Brazing*, pp 140-143, ASM International, Metals Park, OH, 1993.
- [19] M.M. Schwartz, *Ceramic Joining*, pp. 89-93, Metals Park, OH, ASM International, 1990.
- [20] A.K. Jadoon, B. Ralph, and P.R. Hornsby, "Metal to ceramic joining via a metallic interlayer bonding technique," *Journal of Materials Processing Technology*, Vol. 152, No. 3, pp. 257-265, 2004.
- [21] C.A. Walker, V.C. Hodges, "Comparing metal-ceramic brazing methods," *Welding Journal*, No. October, pp. 43-50, 2008.
- [22] H. Mizuhara, "Ceramic-to-Metal Joining: Past, Current and Future," In: P.T. Vianco and M. Singh, eds., *Advanced Brazing and Soldering Technologies*, pp. 278-283, Metals Park, OH, ASM International, 2000.